Filtration characteristics of carbon nanotubes and preparation of buckypapers

Takaaki Tanaka

Department of Materials Science and Technology, Niigata University, Niigata 950-2181, Japan
Tel. +81252627495; Fax +81252627495; email: tctanaka@eng.niigata-u.ac.jp

ABSTRACT

Membrane filtration is often used in purification of carbon nanotubes and in preparation of their thin films (buckypaper). Filtration characteristics of multiwall carbon nanotubes (MWCNT) suspended in aqueous solution of detergents was investigated in this study. Although the diameter of the MWCNT was estimated at around 50 nm from the scanning electron micrograph, a microfiltration membrane whose nominal pore size was 0.2 μm retained the carbon nanotubes. The specific resistance of the filter cake of the carbon nanotubes was 7×10^{13} m kg^{-1} at 98 kPa and the compressibility index was 0.12. The carbon nanotubes were entangled in the buckypaper formed on the microfiltration membrane and the internal structure of the buckypaper was similar under the applied pressure in the preparation of 10–98 kPa.

Keywords: Carbon nanotube; Membrane filtration; Microfiltration; Filtration characteristics; Buckypaper

1. Introduction

Carbon nanotubes [1,2] have received much attention as functional materials [3]. The materials are synthesized via arc discharge [2], laser ablation [4], chemical vapor deposition [5], etc. The raw products usually contain impurities such as amorphous carbon, fullerenes, and catalytic metals. The impurities should be removed to utilize carbon nanotubes efficiently. Most of the amorphous carbon and fullerenes are removed by gas phase oxidation [6]. Fullerenes can also be removed with toluene because they are soluble in the solvent [4]. Then the carbon nantubes are treated by acids such as HCl [6], HNO$_3$ [7], and H$_2$SO$_4$–HNO$_3$ mixtures [8] to remove catalytic metals and residual amorphous carbon. The carbon nanotubes are recovered by centrifugation or filtration after acid treatments. From the viewpoint of production engineering filtration is superior to centrifugation because the former can be easily scaled up.

Filtration is also used to prepare thin carbon nanotube networks, which are used to prepare electric circuits [9] and gas sensors [10,11] by transferring to the surface of plastics, such as polydimethylsiloxane. Thin carbon nanotube films ''buckypapers'' are also prepared by filtration to use them as gas filters [12], electromechanical actuators [13] and electrodes of Li-ion batteries [14] and fuel cells [15]. The carbon nanotube networks are usually formed by vacuum filtration and the filtration characteristics are not studied in detail [12]. However, the speed and energy efficiency is required in the recovery and processing of carbon nanotubes related manufactures.

In this study filtration characteristics of carbon nanotubes were investigated with microfiltration membranes. The dependence the internal structure of buckypapers on the different filtration conditions was also examined.

2. Experimental

2.1. Materials

Multiwall carbon nanotube (MWCNT) suspensions (Meijo Nanocarbon, Nagoya) were mainly used in this study. The nanotubes were suspended in the aqueous detergent solution supplied by the manufacturer.

2.2. Membrane filtration

A filtration cell (Amicon model 8010, 4.1 cm^2, Millipore, Bedford, MA) was used without its stirrer for dead-end filtration experiments. The filtration was performed at a transmembrane pressure of 10 kPa and at 25 ± 2 °C. Cellulose acetate microfiltration membranes with a nominal pore size of 0.20 µm (C020, Advantec, Tokyo), 0.45 µm (C045, Advantec), and 0.80 µm (C080, Advantec) were mainly used in this study. The leakage of nanotubes in permeate was monitored with the absorbance at 660 nm of the initial 10 cm^3 permeate. The absorbance measured with a spectrophotometer (UV-1600, Shimadzu, Kyoto) at 660 nm was proportional to the concentration at least less than 0.01 kg m^{-3}. The proportionality coefficient was 36 m^3 kg^{-1}.

2.3. Scanning electron microscopy (SEM)

The membrane was immersed in liquid nitrogen and then fractured. It was mounted vertically on a sample holder. The surface of the sample was coated with gold using a sputter coater (JFC-1100E, JEOL, Akishima, Japan). A scanning electron microscope (JSM-5800, JEOL) with an accelerating voltage of 15 kV was used to examine the membrane cross-sections and surfaces.

3. Results and discussion

3.1. Effect of membrane pore size

Fig. 1 shows the permeation behavior in filtration of carbon nanotube suspensions with microfiltration membranes with different pore sizes (0.20–0.80 µm). The diameter of the MWCNT was estimated at around 50 nm from the SEM. The microfiltration membrane retained the carbon nanotubes except during the initial stage of filtrations. The permeate from the outlet of the filtration module was black just after the start of the filtration. However, the turbidity became lower as the filtration proceeded. A thin black cake layer formed on the filtration membrane. The reverse side of the membranes was white. The filter papers for supporting the microfiltration membranes were also white after
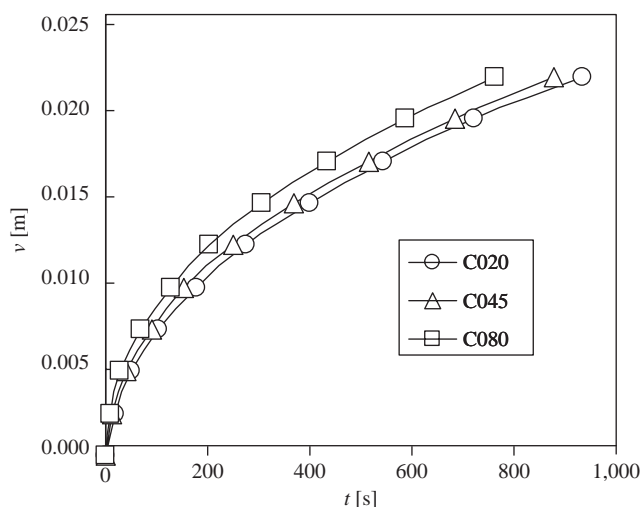

Fig. 1. Permeation behavior of carbon nanotube suspension at 1.00 kg m^{-3} in filtration of different microfiltration membranes. v and t denote the permeation volume per unit filtration area and the filtration time, respectively.

filtration suggesting that the paper did not contain black carbon nanotubes.

Table 1 shows the leakage of carbon nanotubes in filtration with different membranes. The leakage averaged from 0 to 10 cm^3 of permeate volume was less than 1.5% in the filtration at 10 kPa and 1 kg m^{-3}. The cake layer formed on the membrane retained the nanotubes after small amounts of them passed. The leakage increased as the increase of membrane pore size. The membrane resistances (R_m) of the membranes were measured with the dispersion medium by using the following equation,

$$R_m = \frac{\Delta P}{\mu J}, \tag{1}$$

where ΔP, μ, and J are transmembrane pressure, viscosity of permeate, and permeation flux, respectively. The value of the permeate viscosity assumed to nearly equal to that of water at 25°C of 0.89 mPa s [16]. The membrane resistances of C020, C045, and C080 membranes were 3.49, 1.60, and 0.46 nm^{-1}, respectively.

Table 1
Leakage of carbon nanotubes in filtration with microfiltration membranes with different nominal pore sizes. $C = 1.00$ kg m^{-3}; $\Delta P = 10$ kPa

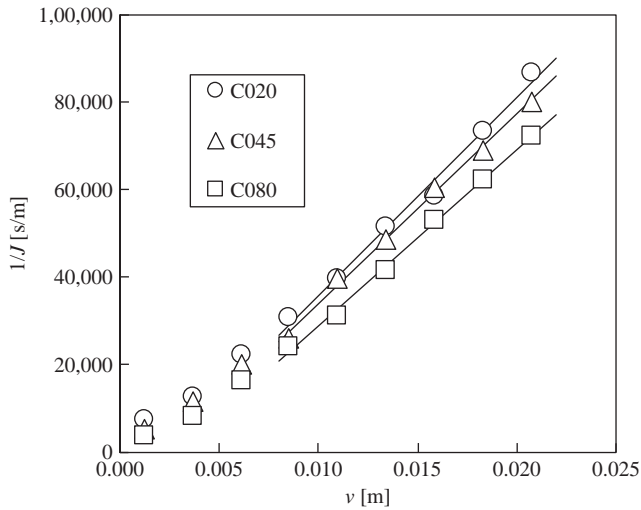| Membrane	Nomnal pore size [µm]	Leakage [%]
C020	0.20	0.26
C045	0.45	0.41
C080	0.80	1.30

Fig. 2. $1/J$ vs. v plot for filtration of carbon nanotube suspensions for Fig. 1. J and v denote permeation flux and permeate volume per unit filtration area, respectively.

However, the permeation flux behaviors were similar after the very initial period. Thus in the following sections we used C020 membrane with a nominal pore size of 0.20 μm because its leakage was the lowest among the membranes.

Fig. 2 shows a plot of the reciprocal of permeation flux $(1/J)$ vs. permeation volume per unit filtration area (v) in the filtrations shown in Fig. 1. It is known that the permeation resistance increases linearly to the permeate volume in cake filtration [17]. In filtration of dilute suspensions the permeation flux follows Eq. (2) in cake filtration.

$$\frac{1}{J} = \frac{\mu(R_m + \alpha C v)}{\Delta P} \tag{2}$$

where α, C, and v are specific resistance of cake, particle concentration, and permeate volume per unit filtration area. The slope of the graph in Fig. 2 corresponds to $\frac{\mu \alpha C}{\Delta P}$. The specific resistances calculated from the slopes were 49.9, 48.7, and 45.4 Tm kg^{-1} for C020, C045, and C080 membranes, respectively. The similar specific resistance suggests that the filter cake formed on the membranes had similar internal structures since the specific resistance highly depends on the porosity (ϵ) of the filter cake [17].

In this study the lowest leakage of carbon nanotubes in microfiltration was attained with the membrane with a nominal pore size of 0.20 μm although its membrane resistance was the highest. The permeation behavior with the membrane in cake filtration is similar to those with the membranes of larger pores. The result in this section suggests that the microfiltration membranes
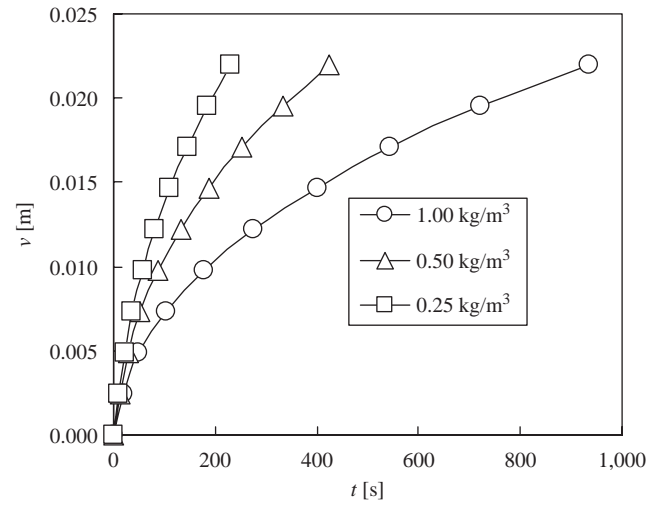

Fig. 3. Permeation behavior of carbon nanotube suspension in filtration at 10 kPa with C020 membranes.

with a nominal pore size of 0.20 μm is one of the best candidates for carbon nanotubes recovery by filtration.

3.2. Effect of carbon nanotube concentration

Fig. 3 shows the permeation behavior of the carbon nanotube suspension at different concentrations. The lower the concentration the faster the permeation proceeded. The leaked nanotube concentration in 10 cm^3 of permeate was 0.0026, 0.0017, and 0.0016 kg m^{-3} at the concentration in feed of 1.00, 0.50, and 0.25 kg m^{-3}, respectively. The lower leaked concentration at lower feed concentration suggests that the amount for the carbon nanotubes necessary to clog the membranes before cake filtration decreased. However the amount was less proportional to the feed concentration. Thus the leakage was higher at lower feed concentrations (Table 2).

Fig. 4 shows the plot of $1/J$ vs. v in the filtrations shown in Fig. 3. The specific resistances calculated from the slopes were 49.9, 43.2, and 37.6 Tm kg^{-1} at 1.00, 0.50, and 0.25 kg m^{-3}, respectively. The lower specific resistance at 0.25 kg m^{-3} suggests that the higher porosity of the filter cake at the concentration although

Table 2
Leakage of carbon nanotubes in filtration of suspensions at different concentrations. Membrane pore size = 0.20 μm; $\Delta P = 10$ kPa

Concentration [kg m^{-3}]	Leakage [%]
1.00	0.26
0.50	0.34
0.25	0.66
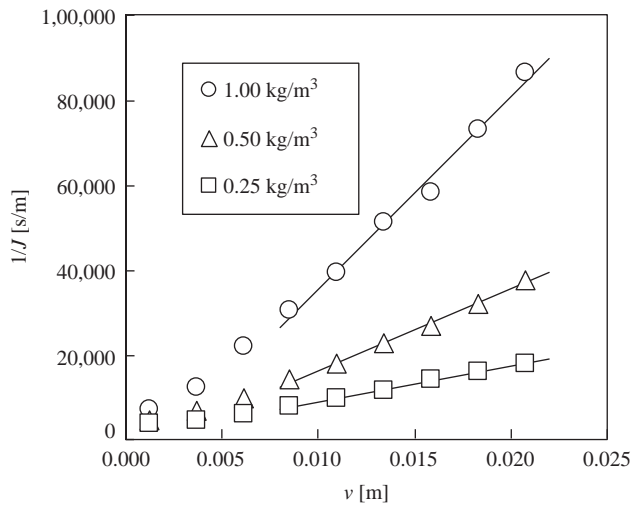
Fig. 4. $1/J$ vs. v plot for filtration of carbon nanotube suspensions for Fig. 3.

Table 3
Leakage of carbon nanotubes in filtration of suspensions at different transmembrane pressures. Membrane pore size = 0.20 μm; $C = 1.00$ kg m^{-3}.

Pressure [kPa]	Leakage [%]
10	0.26
20	0.25
39	0.26
98	0.28

the porosity is nearly proportional to the cubic root of specific resistance at high porosities [17].

Although the specific resistance depended on the concentration the filtration time to a certain permeation volume (e.g., $v = 0.022$ m) was almost proportional to the concentration because the dependence of the specific resistance was low. The proportionality will be helpful for the estimation of filtration time in purification of carbon nanotube by filtration after suspending the nanotubes in different volume of washing solution.

3.3. Effect of transmembrane pressure

Fig. 5 shows the permeation behavior of the carbon nanotube suspension at different transmembrane
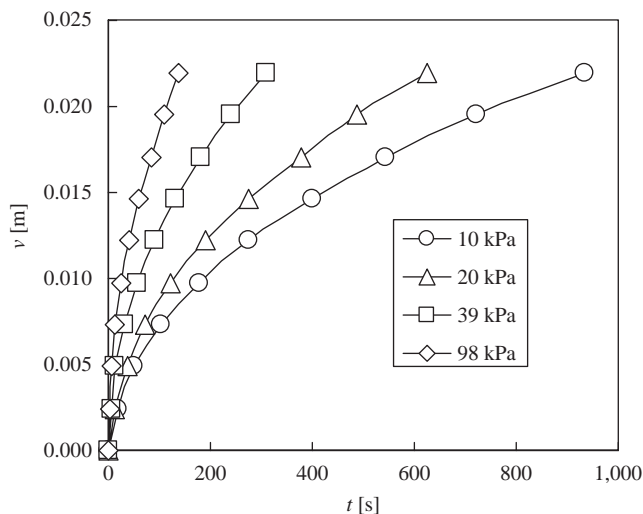
pressures. The permeation proceeded faster at higher transmembrane pressures. The leakage of carbon nanotubes were similar (0.25–0.28%) (Table 3).

Fig. 6 shows the plot of $1/J$ vs. v in the filtrations shown in Fig. 5. The specific resistances calculated from the slopes are shown in Fig. 7. The specific resistance slightly increased with increasing transmembrane pressure. The relationship is often shown by the following equation

$$\alpha = \alpha_1 \cdot (\Delta P)^n, \tag{3}$$

where α_1 and n are the specific resistance at 1 Pa and the compressibility index of the filter cake, respectively. The value of the carbon nanotube used in this study was 0.12. The compressibility index was much lower than the value for the filter cake of rod-shaped microorganisms (0.5–1.0) [18].

The effect of transmembrane pressure on the performance of microfiltration (Figs. 5 and 6, and Table 3) suggests that the recovery of carbon nanotubes and preparation of buckypaper by vacuum (suction)
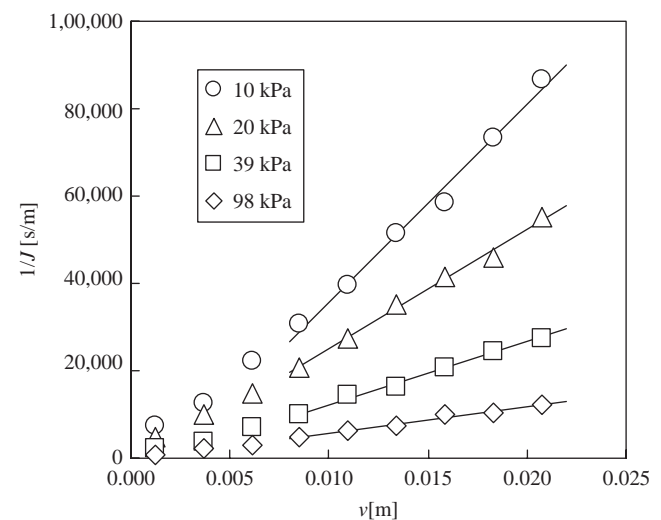

Fig. 5. Permeation behavior of carbon nanotube suspension at 1.00 kg m^{-3}.

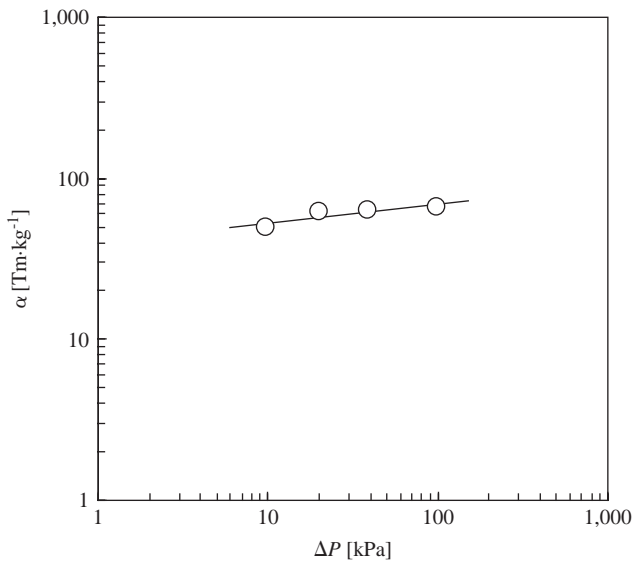Fig. 6. $1/J$ vs. v plot for filtration of carbon nanotube suspensions for Fig. 5.

Fig. 7. Dependence of the specific resistance (α) on the transmembrane pressure (ΔP) of filter cake of carbon nanotube.

filtration are faster when the higher transmembrane pressure is applied.

3.4. Structure of buckypapers

Fig. 8 shows the appearance of the filter cake (buckypaper) formed on the filtration membrane at 10 kPa. The buckypaper easily separated from the microfiltration membrane. Figs. 9 and 10 show the internal
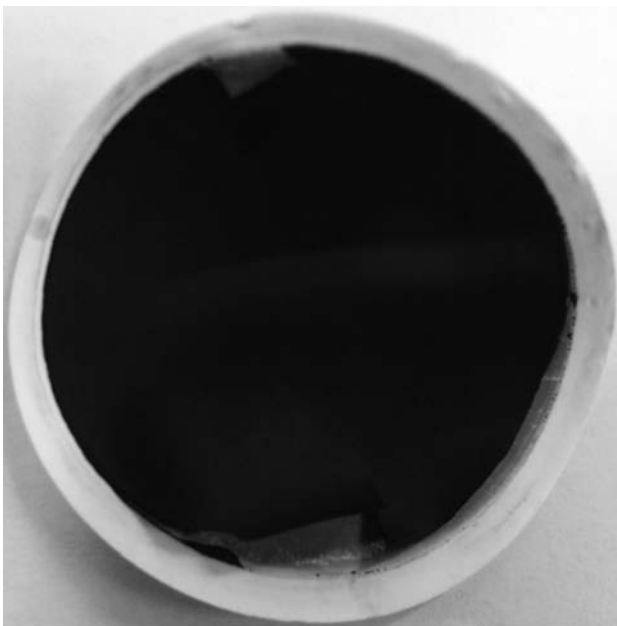

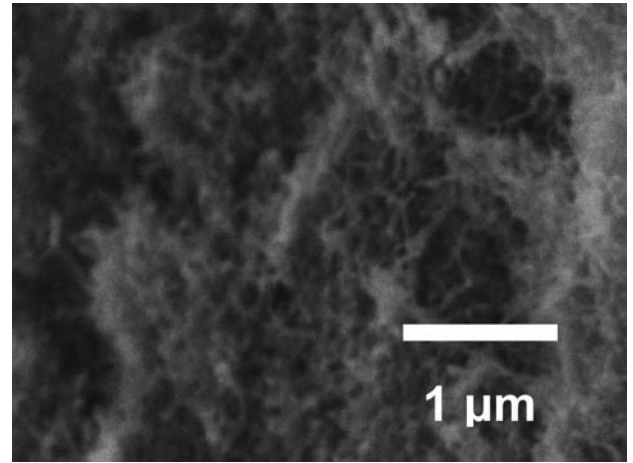Fig. 8. Buckypaper prepared by filtration at a pressure of 10 kPa.

Fig. 9. SEM photographs of cross-sections of buckypaper prepared by filtration at a pressure of 10 kPa.

structure of the buckypaper formed on the filtration membrane. The carbon nanotubes were entangled in the buckypaper although they were homogeneously suspended in the feed suspension. The internal structure of the buckypaper was similar under the applied pressure in the preparation of 10–98 kPa. The low compressibility index (Fig. 7) supports the similarity. The data also suggests that buckypapers having similar structures can be prepared the faster at a higher transmembrane pressure under about 1 atm (= 101 kPa) where the vacuum filtration is usually applied.

4. Conclusions

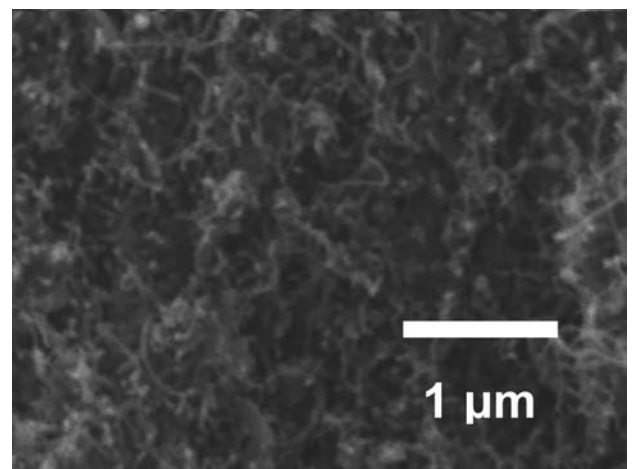MWCNT of a diameter of around 50 nm was recovered a 0.2 μm-pore microfiltration membrane. The

Fig. 10. SEM photographs of cross-sections of buckypaper prepared by filtration at a pressure of 98 kPa.

specific resistance of the filter cake was 7×10^{13} m/kg at 98 kPa and the compressibility index was 0.12. The buckypapers prepared under 10–98 kPa had similar internal structures of entangled nanotubes.

Acknowledgement

Symbols

C	Particle concentration, kg m^{-3}	
J	Permeation flux, m s^{-1}	
n	Compressibility index, –	
R_m	Membrane resistance, m^{-1}	
t	Time, s	
v	Permeate volume per unit filtration area, m	
α	Specific resistance of cake, m kg^{-1}	
α_1	Specific resistance at 1 Pa, m kg^{-1}	
ϵ	Porosity of cake, –	
ΔP	Transmembrane pressure, Pa	
μ	Viscosity of permeate, Pa s	

References

[1] S. Iijima, Helical microtubules of graphitic carbon, Nature, 354 (1991) 56–58.

[2] T.W. Ebbesen and P.M. Ajayan, Large-scale synthesis of carbon nanotubes, Nature, 358 (1992) 220–222.

[3] R.H. Baughman, A.A. Zakhidov, and W.A. de Heer Carbon nanotubes – the route toward applications, Science, 297 (2002) 787–792.

[4] K.B. Shelimov, R.O. Esenaliev, A.G. Rinzler, C.B. Huffman, and R.E. Smalley, Purification of single-wall carbon nanotubes by ultrasonically assisted filtration, Chem. Phys. Lett., 282 (1998) 429–434.

[5] A. Srivastava, O.N. Srivastava, S. Talapatra, R. Vajtai, and P.M. Ajayan, Carbon nanotube filters, Nat. Mater., 3 (2004) 610–614.

[6] Z. Shi, Y. Lian, F. Liao, X. Zhou, Z. Gu, Y. Zhang, and S. Iijima, Purification of single-wall carbon nanotubes, Solid State Commun., 112 (1999) 35–37.

[7] A.C. Dillon, T. Gennett, K.M. Jones, J.L. Alleman, P.A. Parilla, and M.J. Heben, A simple and complete purification of single-walled carbon nanotube materials, Adv. Mater., 11 (1999) 1354–1358.

[8] S. Fogden, R. Verdejo, B. Cottam, and M. Shaffer, Purification of single walled carbon nanotubes: The problem with oxidation debris, Chem. Phys. Lett., 460 (2008) 162–167.

[9] C. Lim, D.H. Min, and S.B. Lee, Direct patterning of carbon nanotube network devices by selective vacuum filtration, Appl. Phys. Lett., 91 (2007) 243117.

[10] A. Modi, N. Koratkar, E. Lass, B. Wei, and P.M. Ajayan, Miniaturized gas ionization sensors using carbon nanotubes, Nature, 424 (2003) 171–174.

[11] S. Chopra, K. McGuire, N. Gothard, A.M. Rao, and A. Pham, Selective gas detection using a carbon nanotube sensor, Appl. Phys. Lett., 83 (2003) 2280.

[12] R. Smajda, A. Kukovecz, Z. Kónya, and I. Kiricsi, Structure and gas permeability of multi-wall carbon nanotube buckypapers, Carbon, 45 (2007) 1176-1184.

[13] D. Suppiger, S. Busato, and P. Ermanni, Characterization of single-walled carbon nanotube mats and their performance as electromechanical actuators, Carbon, 46 (2008) 1085–1090.

[14] S.H. Ng, J. Wang, Z.P. Guo, J. Chen, G.X. Wang, and H.K. Liu, Single wall carbon nanotube paper as anode for lithium-ion battery, Electrochim. Acta, 51 (2005) 23–28.

[15] W. Li, C. Liang, J. Qiu, W. Zhou, H. Han, Z. Wei, G. Sun, and Q. Xin, Carbon nanotubes as support for cathode catalyst of a direct methanol fuel cell, Carbon, 40 (2002) 791–794.

[16] G. Tchobanoglous and F.L. Burton (Eds.), Wastewater Engineering: Treatment and Reuse, 4th ed., p. 1742, McGraw-Hill, New York, NY, 2003.

[17] M. Mulder, Basic Principles of Membrane Technology, 2nd ed., Kluwer Academic Publishers, Dordrecht, The Netherlands, 1996, p. 449.

[18] T. Tanaka, K. Usui, K. Kouda, and K. Nakanishi, Filtration behaviors of rod-shaped bacterial broths in unsteady-state phase of cross-flow filtration, J. Chem. Eng. Jpn., 29 (1996) 973–981.